

Self-Assembly of Tricuprous Double Helicates: Thermodynamics, Kinetics, and Mechanism

by Nicolas Fatin-Rouge^a), Sylvie Blanc^a), Armin Pfeil^b), Annie Rigault^b), Anne-Marie Albrecht-Gary^{*a}), and Jean-Marie Lehn^{*}

^a) Laboratoire de Physico-Chimie Bioinorganique, UMR 7509 du CNRS, Faculté de Chimie, 1 rue Blaise Pascal, F-67000 Strasbourg

^b) Laboratoire de Chimie Supramoléculaire, ISIS, Université Louis Pasteur, 4 rue Blaise Pascal, F-67000 Strasbourg

Dedicated to *Edgar Heilbronner* on the occasion of his 80th birthday

We report in this paper the coordination and kinetic properties of two oligobipyridine strands, which contain three 2,2'-bipyridine subunits separated by oxydimethylene bridges, the 4,4'-bis(CONET₂)-substituted **L** and the 4,4'-bis(CO₂Et)-substituted **L'**. Spectrophotometric measurements allowed the characterization of thermodynamic complexes and kinetic intermediates* which are involved in the self-assembly process of **L**₂Cu₃ and **L'**₂Cu₃ helicates. The reaction presents positive cooperativity for the binding of two 2,2'-bipyridine strands to the cuprous cations. While reactive kinetic intermediates* present distorted coordination geometries around Cu^I, the final rearrangement of the tricuprous bistranded helicates allows more closely tetrahedral coordination of each cation and reduces the interactions. Differences in the bulkiness and electronic properties of the **L** and **L'** substituents do not affect significantly the stability of the corresponding helicates, but greatly influence binding rates in the self-assembly process.

Introduction. – In recent years, creating molecules that are programmed by virtue of their structure and binding sites to spontaneously organize themselves into supramolecular architectures held together by metal coordination has aroused the interest of chemists [1–5] (for recent reviews on metal-ion-mediated self-assembly, see, e.g., [2]). Using metal template strategy, helicates [6–16], ladder [17], grids [18], rings [2][3][19], cages [2][3][20], catenates, and knots [21–23], were generated. To design such species presenting specific structural and functional features, it is of great importance to establish the rules by which control the assembly process can be achieved through chemical programming by means of suitable components and assembling algorithms [1][5]. In the self-assembly of helicates, three main structural features determine the nature and shape of the helical species formed. The binding sites impose the number of strands able to coordinate metal ions with a given geometry. Bidentate or tridentate subunits combined, respectively, with metal ions of tetrahedral [6][7] and of octahedral [6][24] coordination geometry produce double helical polynuclear species, while triple helical complexes are formed with bidentate ligands and octahedrally coordinated metal ions [25]. Taking into account these properties, double-helical mixed-valence [14] heteronuclear [26] or heterostranded [27] complexes have been synthesized. However, not every combination of oligomultidentate ligands with metal ions will give helical structures, and the spacers between the metal binding sites play an important role. They should be flexible enough to allow the ligand to bind

strongly to the metal ion, and rigid enough to limit the number of conformations and favor interstrand over intrastrand binding. Finally, helicity implies that all metal centers must have the same screw sense and the same configuration at the metal centers. The family of double-stranded helicates generated from ligands with multiple diimine binding domains and transition-metal ions of various binding geometries presents such properties. However, if their structures are well characterized by crystallography [6][7][28], NMR [6][7][29], mass spectrometry [30][31], or electrochemistry [32], few physico-chemical properties are available in the literature [33][34]. Spectrophotometric and thermodynamic parameters of triple helical lanthanide complexes have been reported [35]. Thermodynamic cooperativity was studied on double-stranded Cu^I [36] and Ag^I [37] trinuclear helicates. More recently, the stability constants of anchored triple ferric helicates in MeOH have been determined [38]. The formation mechanism of such structures has been investigated [39][40], but further information on the parameters involved in the complexation process are required.

We report in this paper the coordination and kinetic properties of two oligobipyridine strands derived from the initial double helicate forming ligand [7] containing three 2,2'-bipyridine (bipy) subunits separated by oxydimethylene bridges, the 4,4'-bis(CONEt₂)-substituted **L** [41] and the 4,4'-bis(CO₂Et)-substituted **L'** [42] (Fig. 1). By means of classical spectrophotometric titrations and electrospray mass spectrometric (ES-MS) measurements, we have investigated the nature of the species that they form with Cu^I, and determined their respective stability constants and absorption spectra to gain insight into the distribution of the different species at a given ligand/Cu^I ratio and into the physicochemical and mechanistic features of their self-assembly process. The formation kinetics of Cu^I complexes with **L** and **L'** have been investigated under the same experimental conditions by single and multiwavelength absorption spectrophotometry with fast mixing technique. A similar behavior has been observed for both ligands; however, the rate constants are very sensitive to structural changes.

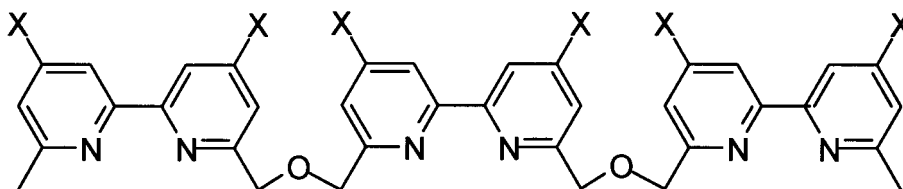


Fig. 1. Structure of ligands **L** (X = CONEt₂) [40] and **L'** (X = CO₂Et) [42].

Experimental. – Materials. Ligands **L** and **L'** were synthesized according to previously published procedures [41], and [Cu(CH₃CN)₄][BF₄] was prepared according to the method in [43]. The solvent selected for this work was a ternary mixture of solvents, MeCN/H₂O/CH₂Cl₂ 80:15:5 (v/v), in which the ligands (CH₂Cl₂, Merck, Uvasol), the copper salt (MeCN, Merck, Uvasol), and Et₄NCN (H₂O, Fluka), which was used for decomplexation studies, are soluble. The solvent was deaerated and protected from light. The ligand and cuprous stock solns. were prepared by accurate weighing. The ionic strength was fixed at 0.1M with tetrabutylammonium trifluoromethanesulfonate (Fluka, puriss).

Electrospray-Mass-Spectrometric Measurements. ES Mass spectra (Fig. 2) were obtained on a VG BioQ triple-quadrupole with a mass to charge (*m/z*) range of 4000 (VGBioTech Ltd., Altrincham, UK). The ES interface was heated to 70°. The sampling cone voltage (*V_c*) was 20 V. No fragmentation process was observed at this voltage. The calibration was performed using multiprotonated ions from horse myoglobin. The resolution

was about 600 at m/z 1000 (with a valley of 10%), and then average masses were measured. Scanning was performed from m/z 400 to 1400 in 10 s. The data system was operated as a multichannel analyzer, and several scans were summed to obtain the final spectra. Solns. containing the ligand **L** (1.2×10^{-4} M), and 0.2, 0.5, 1.0, 5.0, and 20.0 equiv. of Cu^{I} in $\text{MeCN}/\text{H}_2\text{O}/\text{CH}_2\text{Cl}_2$ (80:15:5), resp., were injected into the mass spectrometer source with a syringe pump (Harvard type 55 1111, Harvard Apparatus Inc., South Natick, MA, USA) at a flow rate of 4 ml/min.

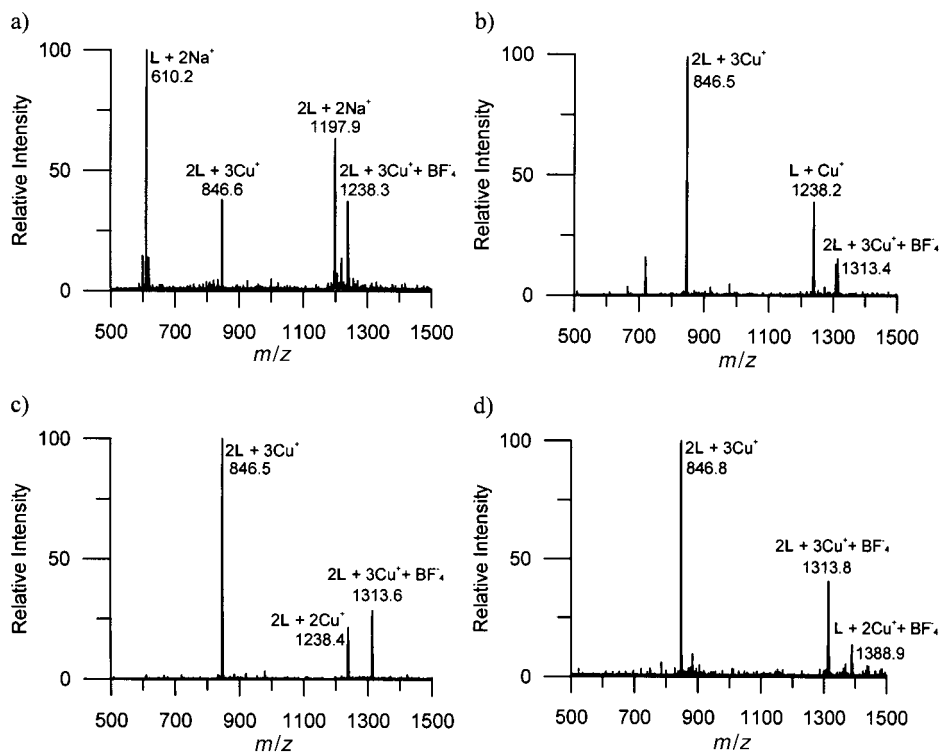


Fig. 2. Electro spray mass spectra. a) $[\text{Cu}^{\text{I}}]_{\text{tot}}/[\text{L}]_{\text{tot}} = 0.1$; b) 0.5; c) 1.0; d) 20; positive mode $[\text{L}]_{\text{tot}} = 1.2 \times 10^{-4}$ M. Solvent: $\text{MeCN}/\text{H}_2\text{O}/\text{CH}_2\text{Cl}_2$, 80:15:5.

Spectrophotometric Measurements. Titrations were carried out in 5-ml volumetric flasks using a precision piston microburet (Gilmont) to add Cu^{I} and the free ligand **L**. Between 18 and 24 solns. were prepared with a $[\text{Cu}^{\text{I}}]_{\text{tot}}/[\text{ligand}]_{\text{tot}}$ ratio ranging between 0 and 1000. The ligand **L** concentration was first fixed at 1.2×10^{-4} M and Cu^{I} concentrations were varied between 0 and 2.4×10^{-3} M. The Cu^{I} concentration was then fixed at 4.46×10^{-3} M, and ligand concentrations were varied between 2.6×10^{-6} and 2.6×10^{-4} M. Another titration was performed in excess of ligand **L** (6.7×10^{-4} M) with the Cu^{I} concentrations varying between 6.9×10^{-6} and 6.83×10^{-5} M. UV/VIS (260–650 nm) absorption spectra were recorded on an Uvikon 941 (Kontron) spectrophotometer equipped with 0.2; 1- or 2-cm quartz cells (Hellma), and thermostated at 25.0 (1)°. A typical set of spectra is given in Fig. 3.

The spectrophotometric data were analyzed with both the *Letagrop-Spefo* [44–46] and *Specfit* [47–50] programs, by which the absorptivities and the stability constants of the species formed at equilibrium were adjusted. The *Letagrop-Spefo* program uses the *Newton-Raphson* algorithm to solve mass-balance equations and a pit-mapping method to minimize the errors and determine the best parameter values. *Specfit* uses factor analysis to reduce the absorbance matrix and to extract the eigenvalue prior to the multiwavelength fit of the reduced data set according to the *Marquardt* algorithm [51][52].

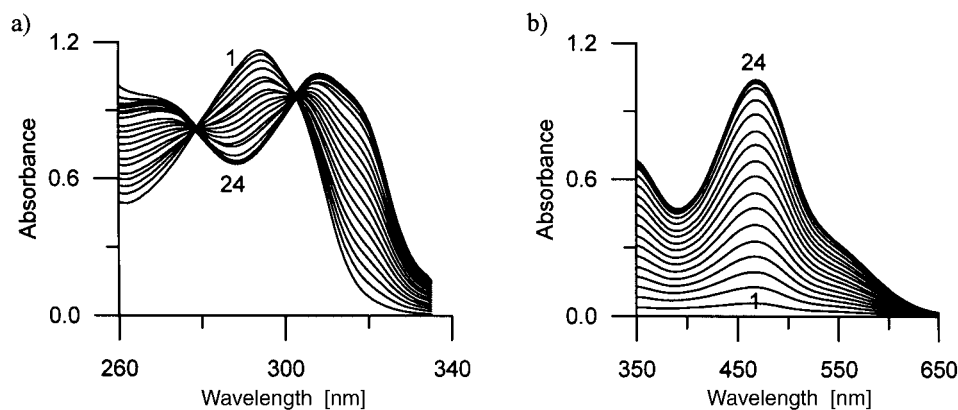


Fig. 3. Absorption spectra of **L** with varying Cu^{I} concentrations. Solvent: MeCN/ H_2O / CH_2Cl_2 , 80:15:5 (v/v); $T = 25.0(2)^\circ$; $I = 0.1$; a) $l = 0.2$ cm; b) $l = 1$ cm; $[\text{L}]_{\text{tot}} = 1.2 \times 10^{-4}$ M; 1–24: $[\text{Cu}^{\text{I}}]_{\text{tot}} \times 10^5$ M = 0; 1.2; 2.4; 3.6; 4.8; 6.0; 7.2; 8.4; 9.6; 10.8; 12.0; 13.2; 14.4; 15.6; 16.8; 18.0; 19.2; 20.4; 21.6; 22.8; 24; 59.9; 119.9; 240.0 M, resp.

Formation Kinetics of the Trinuclear Cuprous Helicates of L and L'. The reactions of Cu^{I} with ligands **L** and **L'** at $25.0(1)^\circ$ involve rapid steps which were recorded on an *Applied Photophysics* stopped-flow *SX-18MV* spectrophotometer. Pseudo-first-order conditions with respect to the ligands (2.5×10^{-5} M) were used, and Cu^{I} concentrations were varied between 2.5×10^{-4} and 2×10^{-3} M. Experiments with excess of **L'** (1.449×10^{-4} M; 8.69×10^{-4} M; 5.80×10^{-4} M, and 2.90×10^{-4} M) were also undertaken in MeCN/ CH_2Cl_2 80:20 (v/v) with a low concentration of Cu^{I} (5.8×10^{-6} M). The data sets, averaged out of at least three replicates and recorded with a 1-cm path length at the absorption maximum of the LMCT band, were analyzed on-line with the commercial software *Biokine* [53]. This program fits up to three exponential functions to the experimental curves with the *Simplex* algorithm [54] after initialization with the *Padé-Laplace* method [55]. The second-order rate constants were calculated by non-weighted linear regression using the commercial *Enzfitter* program [56] based on *Marquard* [51] analysis. Time-resolved absorption spectra were also collected between 300 and 450 nm with a 1-cm path length. The rate constants and the extinction coefficients were adjusted to the multiwavelength data sets by nonlinear least-squares analysis with the *Specfit* program [47–50].

Results. – Thermodynamics and Spectrometry. The ES mass spectra recorded at various $[\text{Cu}^{\text{I}}]_{\text{tot}}/[\text{L}]_{\text{tot}}$ ratios (Fig. 2) indicate the formation of four complexes: **LCu**, **LCu₂**, **L₂Cu₂**, and **L₂Cu₃** (available as *Supplementary Material*). They also reveal that the double helicate **L₂Cu₃** is already the major product at a $[\text{Cu}^{\text{I}}]_{\text{tot}}/[\text{L}]_{\text{tot}}$ ratio of 0.5, well below the stoichiometric value of 1.5.

Spectrophotometric titrations of **L** with Cu^{I} (Fig. 3) were carried out to calculate the binding constants of the complexes and to determine the corresponding electronic spectra (260–650 nm). The best fit of the spectrophotometric data was obtained by both *Specfit* [47–50] and *Letagrop-Spefo* [44–46] programs with a model including three complexes observed by ES-MS (**LCu**, **L₂Cu₂**, and **L₂Cu₃**), **LCu₂** having not been characterized under our experimental conditions. The values of the global stability constants obtained are summarized in *Table 1*.

The absorption spectra of the Cu^{I} complexes are dominated by a ligand-to-metal charge transfer band (LMCT) in the visible region ($\lambda_{\text{max}} = 460\text{--}470$ nm). Using the stability constants presented in *Table 1*, the corresponding distribution curves were calculated with the *Haltafall* program [57]. Fig. 4, a, shows in agreement with the ES-

Table 1. *Global Stability Constants and Spectrophotometric Parameters for the Cuprous Complexes Formed with L^a) and L^b)*

Equilibrium	$\log \beta(3\sigma)$	λ_{\max} [nm]	ϵ_{\max} [M ⁻¹ cm ⁻¹]
$\mathbf{L} + \text{Cu}^{\text{I}} \rightleftharpoons \mathbf{LCu}$	$\log \beta_{\mathbf{LCu}} = 4.2(1)$	468	6800
$2 \mathbf{L} + 2\text{Cu}^{\text{I}} \rightleftharpoons \mathbf{L}_2\text{Cu}_2$	$\log \beta_{\mathbf{L}_2\text{Cu}_2} = 12.9(3)$	468	14000
$2 \mathbf{L} + 3 \text{Cu}^{\text{I}} \rightleftharpoons \mathbf{L}_2\text{Cu}_3$	$\log \beta_{\mathbf{L}_2\text{Cu}_3} = 18.7(3)$	468	17000
$\mathbf{L}' + \text{Cu}^{\text{I}} \rightleftharpoons \mathbf{L}'\text{Cu}$	$\log \beta_{\mathbf{L}'\text{Cu}} = 4.6(2)$	500	7700
$2 \mathbf{L}' + \text{Cu}^{\text{I}} \rightleftharpoons \mathbf{L}'_2\text{Cu}$	$\log \beta_{\mathbf{L}'_2\text{Cu}} = 8.2(2)$	500	8500
$2 \mathbf{L}' + 2\text{Cu}^{\text{I}} \rightleftharpoons \mathbf{L}'_2\text{Cu}_2$	$\log \beta_{\mathbf{L}'_2\text{Cu}_2} = 13.5(2)$	500	16000
$2 \mathbf{L}' + 3 \text{Cu}^{\text{I}} \rightleftharpoons \mathbf{L}'_2\text{Cu}_3$	$\log \beta_{\mathbf{L}'_2\text{Cu}_3} = 18.6(1)$	500	26000

^a) Solvent: MeCN/H₂O/CH₂Cl₂ 80 : 15 : 5 (v/v); $T = 25.0(2)^\circ$; $I = 0.1$. ^b) Solvent: MeCN/CH₂Cl₂ 50 : 50 (v/v) [36]. The errors are estimated to 1 nm for the wavelengths and to 5% for the extinction coefficients. For the sake of simplicity, charges have been omitted in all the chemical equilibria.

MS data the formation of the trinuclear helicate $\mathbf{L}_2\text{Cu}_3$ in competition with two minor cuprous complexes \mathbf{LCu} and $\mathbf{L}_2\text{Cu}_2$. *Fig. 4, b* and *c*, correspond to the experimental conditions chosen for kinetic measurements in excess of Cu^{I} and in excess of ligand \mathbf{L}' , respectively.

Formation Kinetics of L Cuprous Complexes. Kinetic measurements were carried out in an excess of Cu^{I} with respect to the concentration of \mathbf{L} . A large loss of spectrophotometric amplitude (30% of the total amplitude) was observed during the dead time (3 ms) of the stopped-flow device. Under pseudo-first-order conditions with respect to Cu^{I} , three exponential spectrophotometric signals were recorded at 468 nm in the time range of s and min. For simplicity, the different *Steps* are successively denoted 1, 2, 3, and 4, as indicated in *Fig. 5*. The values of the corresponding pseudo-first-order rate constants $k_{2,\text{obs}}$, $k_{3,\text{obs}}$, and $k_{4,\text{obs}}$ were determined [53] (available as *Supplementary Material*).

With a diode arrays device, we could confirm the three rate-limiting steps. The most striking feature observed in *Fig. 6* is the presence of two absorption bands centered at *ca.* 380 and 560 nm. These bands were not observed at equilibrium (*Fig. 3*) and strongly suggest that reactive kinetic intermediates* are involved in the self-assembly process of $\mathbf{L}_2\text{Cu}_3$. For that reason, all the Cu^{I} species involved in the proposed mechanism are written with an asterisk (*).

The variations of the absorbance $A_{1,\infty}$, measured at 468 nm and at the beginning of the second step, after the initial loss of spectrophotometric amplitude (available as *Supplementary Material*) vs. the analytical concentrations in \mathbf{L} and Cu^{I} suggest the rapid formation of two Cu^{I} species with a single strand \mathbf{L} in two successive reactions:



This reaction scheme leads to the following equations and to the determination of $\epsilon_{\mathbf{LCu}^*}$, $\beta_{\mathbf{LCu}^*}$, $\epsilon_{\mathbf{LCu}_2^*}$, and $\beta_{\mathbf{LCu}_2^*}$:

$$A_{2,0} = \epsilon_{\mathbf{LCu}^*} \times [\mathbf{LCu}^*] + \epsilon_{\mathbf{LCu}_2^*} \times [\mathbf{LCu}_2^*] \quad (3)$$

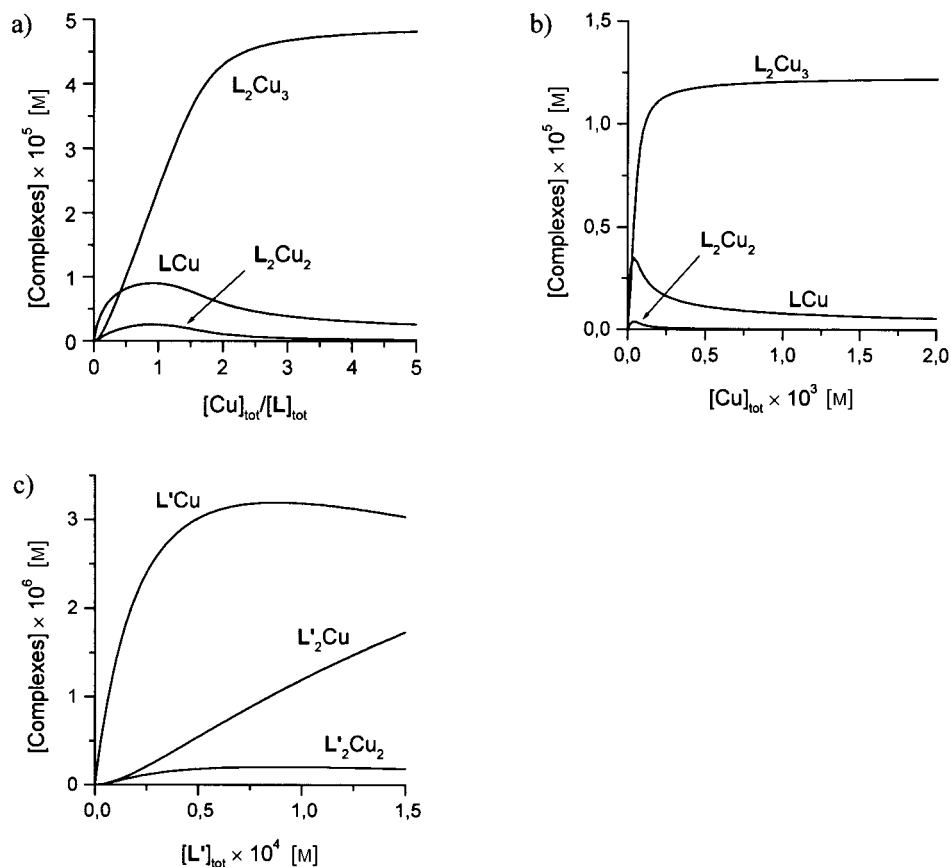


Fig. 4. Distribution curves related to the formation of Cu^{I} complexes with **L**. a) $[\text{L}]_{\text{tot}} = 10^{-4} \text{ M}$, b) $[\text{L}]_{\text{tot}} = 2.5 \times 10^{-5} \text{ M}$, and with **L'**, c) $[\text{Cu}^{\text{I}}]_{\text{tot}} = 5.7 \times 10^{-6} \text{ M}$. Solvent: MeCN/ H_2O / CH_2Cl_2 , 80:15:5 (v/v) except for c) MeCN/ CH_2Cl_2 50:50 (v/v); $T = 25.0^\circ$; $I = 0.1$; the stability constants are given in Table 1.

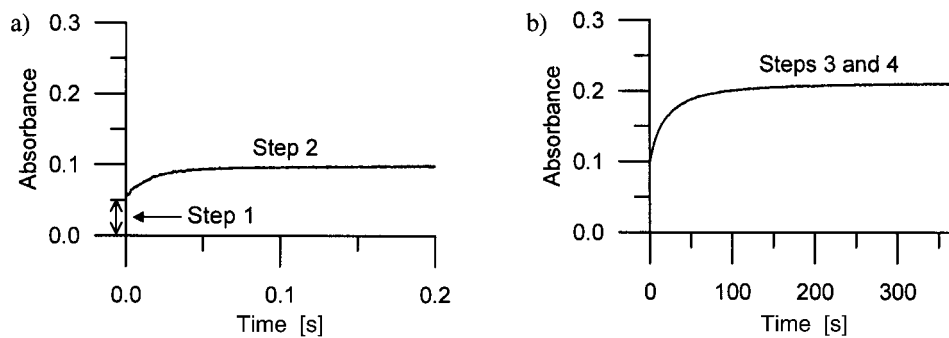


Fig. 5. Evolution of the absorption observed for the formation kinetics of the Cu^{I} complexes with **L** vs. time. Solvent: MeCN/ H_2O / CH_2Cl_2 , 80:15:5 (v/v); $T = 25.0(2)^\circ$; $I = 0.1$; $[\text{L}]_{\text{tot}} = 2.5 \times 10^{-5} \text{ M}$; $[\text{Cu}^{\text{I}}]_{\text{tot}} = 3.1 \times 10^{-4} \text{ M}$; $l = 1 \text{ cm}$; $\lambda = 468 \text{ nm}$.

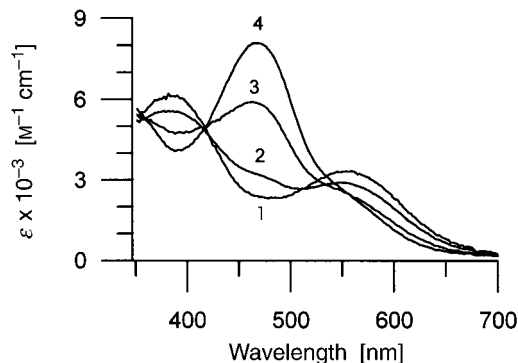


Fig. 6. Time-resolved electronic spectra recorded for the formation of the Cu^{I} complexes of **L**. Solvent: MeCN/ $\text{H}_2\text{O}/\text{CH}_2\text{Cl}_2$, 80:15:5 (v/v); $T=25.0(2)^\circ$; $I=0.1$; $[\mathbf{L}]_{\text{tot}}=2.5 \times 10^{-5} \text{ M}$; $l=1 \text{ cm}$; $[\mathbf{L}]=2.5 \times 10^{-5} \text{ M}$; $[\text{Cu}^{\text{I}}]=2.5 \times 10^{-4} \text{ M}$; $t_1=2.5 \text{ ms}$ and $t_4=500 \text{ s}$.

$$A_{1,\infty} = \frac{[\mathbf{L}]_{\text{tot}} \times [\text{Cu}]_{\text{tot}}}{(1 + \beta_{\text{LCu}^*} \times [\text{Cu}]_{\text{tot}} + \beta_{\text{LCu}_2^*} \times [\text{Cu}]_{\text{tot}}^2)} (\beta_{\text{LCu}^*} \times \epsilon_{\text{LCu}^*} + \beta_{\text{LCu}_2^*} \times \epsilon_{\text{LCu}_2^*} \times [\text{Cu}]_{\text{tot}}) \quad (4)$$

In the second step, a decrease of the corresponding pseudo-first-order rate constant $k_{2,\text{obs}}$ was observed when Cu^{I} concentrations increased. We propose that this step could involve the binding of a second strand to the dicuprous species LCu_2^* rapidly formed:



According to this reaction scheme, the expression of $k_{2,\text{obs}}$ can be written as:

$$k_{2,\text{obs}} = \frac{4 \times k_2 \times \beta_{\text{LCu}_2^*} \times [\mathbf{L}]_{\text{tot}} \times [\text{Cu}]_{\text{tot}}^2}{(1 + \beta_{\text{LCu}^*} \times [\text{Cu}]_{\text{tot}} + \beta_{\text{LCu}_2^*} \times [\text{Cu}]_{\text{tot}}^2)^2} + k_{-2} \quad (6)$$

At the end of this second step, the term $[\text{L}_2\text{Cu}_2^*]_{\infty}^2 - [\text{L}_2\text{Cu}_2^*]^2$ was neglected.

The values of the rate constants k_2 and k_{-2} were determined by a non-linear least-squares methods (Fig. 7, a) and are given in Table 2. The variations of $A_{2,\infty}$ measured at 468 nm at the end of Step 2 (Eqn. 7) are available as Supplementary Material and lead to the determination of $\epsilon_{\text{L}_2\text{Cu}_2^*}$, $\beta_{\text{L}_2\text{Cu}_2^*}$ being equal to $(k_2/k_{-2}) \times \beta_{\text{LCu}_2^*}$.

$$A_{2,\infty} = \frac{[\mathbf{L}]_{\text{tot}} \times [\text{Cu}]_{\text{tot}}}{(1 + \beta_{\text{LCu}^*} \times [\text{Cu}]_{\text{tot}} + \beta_{\text{LCu}_2^*} \times [\text{Cu}]_{\text{tot}}^2)} \times \left(\beta_{\text{LCu}^*} \times \epsilon_{\text{LCu}^*} + \epsilon_{\text{LCu}_2^*} \times \beta_{\text{LCu}_2^*} \times [\text{Cu}]_{\text{tot}} + \frac{\epsilon_{\text{L}_2\text{Cu}_2^*} \times \beta_{\text{L}_2\text{Cu}_2^*} \times [\mathbf{L}]_{\text{tot}} \times [\text{Cu}]_{\text{tot}}}{(1 + \beta_{\text{LCu}^*} \times [\text{Cu}]_{\text{tot}} + \beta_{\text{LCu}_2^*} \times [\text{Cu}]_{\text{tot}}^2)} \right) \quad (7)$$

The variations of the observed rate constant $k_{3,\text{obs}}$ with the Cu^{I} concentration, suggest that a third Cu^{I} cation binds to the dinuclear double-stranded complex L_2Cu_2^*

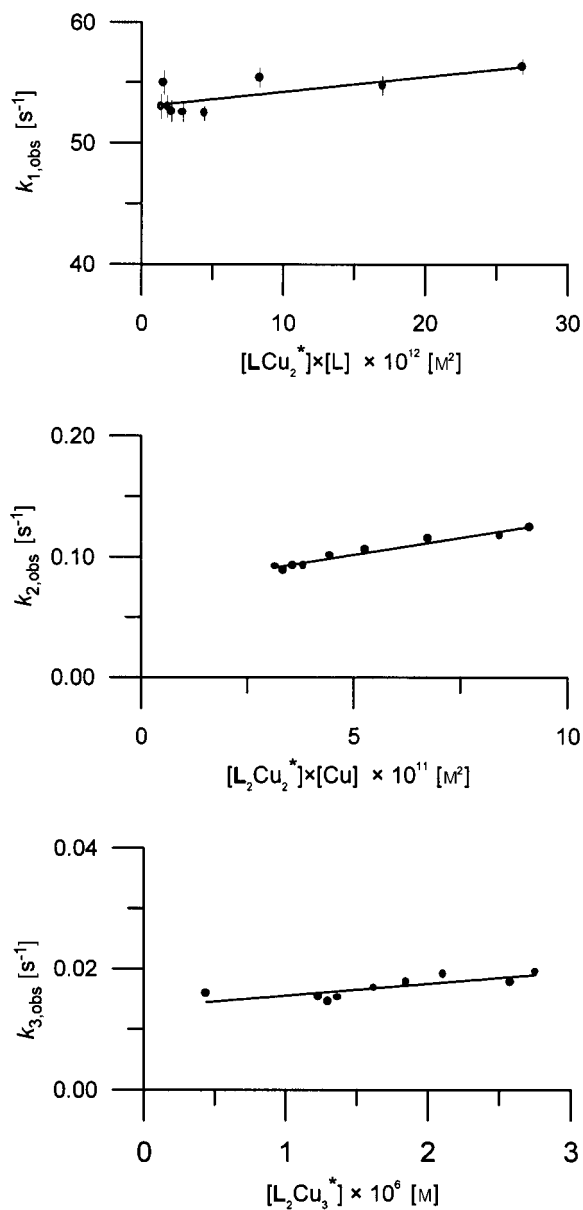


Fig. 7. Variation of the a) first, b) second, and c) third pseudo-first-order constants for the formation of Cu^I complexes of **L** vs. the concentrations of the Cu^I reacting species. Solvent: MeCN/H₂O/CH₂Cl₂, 80:15:5 (v/v); $T = 25.0(2)^\circ$; $I = 0.1$; $[L]_{tot} = 2.5 \times 10^{-5}$ M.

during the third rate-limiting step:



The kinetic data fit well with the following equation which corresponds to the proposed mechanism (*Fig. 7,b*) and leads to the determination of k_3 and k_{-3} (*Table 2*).

$$k_{3,\text{obs}} = \frac{4 \times k_3 \times \beta_{\mathbf{L}_2\text{Cu}_2^*} \times [\mathbf{L}]_{\text{tot}} \times [\text{Cu}]_{\text{tot}}^3}{(1 + \beta_{\mathbf{LCu}^*} \times [\text{Cu}]_{\text{tot}} + \beta_{\mathbf{LCu}_2^*} \times [\text{Cu}]_{\text{tot}}^2)^2} + k_{-3} \quad (9)$$

The fourth and slowest step can be considered as a final rearrangement of the trinuclear double-stranded intermediate*:



The corresponding variations of the pseudo-first-order rate constant $k_{4,\text{obs}}$ vs. the analytical concentrations in \mathbf{L} and in Cu^{I} are expressed by the following equation:

$$k_{4,\text{obs}} = \frac{4 \times k_4 \times \beta_{\mathbf{L}_2\text{Cu}_3^*} \times [\mathbf{L}]_{\text{tot}} \times [\text{Cu}]_{\text{tot}}^3}{(1 + \beta_{\mathbf{LCu}^*} \times [\text{Cu}]_{\text{tot}} + \beta_{\mathbf{LCu}_2^*} \times [\text{Cu}]_{\text{tot}}^2)^2} + k_{-4} \quad (11)$$

As for the other previous steps, the term $[\mathbf{L}_2\text{Cu}_3^*]^2 - [\mathbf{L}_2\text{Cu}_3^*]_{\infty}^2$ was neglected. A statistical treatment by a nonlinear least-squares method leads to the k_4 and k_{-4} values (*Fig. 7,c*), which are presented in *Table 2* with their standard deviations.

Time-resolved absorption spectra were recorded from 350–700 nm. The set of spectra displayed in *Fig. 6* shows a maximum at 558 nm during the first stage, which undergoes a 100-nm blue shift during the following steps. Factor analysis of the entire spectrophotometric data set confirmed the presence of four absorbing species. A satisfactory least-squares fit of the apparent rate constants and absorptivities can be obtained with the previous scheme of successive *Reaction Steps 1, 2, 5, 8, 10*.

Formation Kinetics in Excess of Cu^{I} Complexes of \mathbf{L}' . Kinetic experiments were carried out for \mathbf{L}' in excess of either Cu^{I} (*Table 3*) or ligand (*available as Supplementary Material*). The same mechanism as observed for \mathbf{L} was found. The corresponding rate constants for each of the three rate-determining steps are given in *Table 2*.

In excess of ligand \mathbf{L}' , two monocuprous species $\mathbf{L}'\text{Cu}$ and $\mathbf{L}'_2\text{Cu}$ are formed at equilibrium as shown by the distribution curves (*Fig. 4*). A single exponential signal was observed at 500 nm. The corresponding pseudo-first-order rate constant $k_{1,\text{obs}}$ varies linearly with the analytical concentration of \mathbf{L}' . The values of the first- and second-order-rate constants, which correspond to the ordinate at the origin and to the slope of the line, are calculated by linear regression and are $k_1 = 1.7(6) \times 10^3 \text{ M}^{-1} \text{ s}^{-1}$ and $k_{-1} = 0.22(5) \text{ s}^{-1}$, respectively (*Table 2*).

Discussion. – *Characterization of Cu^{I} Complexes of Ligands \mathbf{L} and \mathbf{L}' .* Depending on the ratio $[\text{Cu}^{\text{I}}]_{\text{tot}}/[\mathbf{L}]_{\text{tot}}$, three thermodynamic cuprous complexes, \mathbf{LCu} , $\mathbf{L}_2\text{Cu}_2$, and $\mathbf{L}_2\text{Cu}_3$, which are of the same stoichiometry as the species observed with \mathbf{L}' in MeCN/ $\text{H}_2\text{O}/\text{CH}_2\text{Cl}_2$ [36], were characterized in MeCN/ $\text{H}_2\text{O}/\text{CH}_2\text{Cl}_2$ 80:15:5 by absorption spectrophotometry (*Fig. 3*) and ES-MS (*Fig. 2*). In a large excess of Cu^{I} , \mathbf{LCu}_2 was detected by ES-MS, but not by absorption spectrophotometry (*Fig. 2,d*). The stability of the three cuprous \mathbf{L} and \mathbf{L}' complexes were characterized at equilibrium, the mononuclear monostranded complex, and the dinuclear and trinuclear bistranded species (*Table 1*). For comparison, collected thermodynamic and spectrophotometric

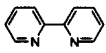
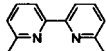
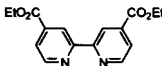
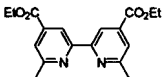
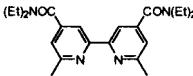
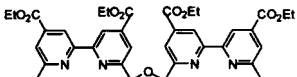
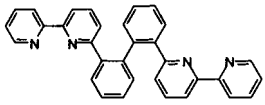
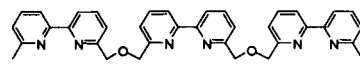
Table 2. Kinetic and Thermodynamic Parameters Determined for the Formation of Cu^I Complexes of L^a and L'^b

Rate-limiting step		Kinetic results
<i>Step 1</i>		
$L + Cu \xrightleftharpoons{\beta_{LCu^*}} LCU$	L	$\log \beta_{LCu^*} = 3.6(4)$ $\log \beta_{LCu_2^*} = 8.1(3)$
$LCu^* + Cu \xrightleftharpoons{K_{LCu^*}} LCu_2^*$	L'	$\log \beta_{LCu^*} = 4.0(5)$ $\log \beta_{LCu_2^*} = 8.0(5)$
<i>Step 2</i>		
$LCu_2^* + L \xrightleftharpoons[k_{-2}]{k_2} L_2Cu_2^*$	L	$k_2 = 7(3) \times 10^5 \text{ M}^{-1} \text{ s}^{-1}$ $k_{-2} = 53.0(6) \text{ s}^{-1} \Rightarrow \log \beta_{L_2Cu_2^*} = 12.2(6)$
	L'	$k_2 = 2.0(7) \times 10^5 \text{ M}^{-1} \text{ s}^{-1}$ $k_{-2} = 0.6(2) \text{ s}^{-1} \Rightarrow \log \beta_{L_2Cu_2^*} = 13.5(6)$
<i>Step 3</i>		
$L_2Cu_2^* + Cu \xrightleftharpoons[k_{-3}]{k_3} L_2Cu_3^*$	L	$k_3 = 1.0(1) \times 10^3 \text{ M}^{-1} \text{ s}^{-1}$ $k_{-3} = 7.2(4) \times 10^{-2} \text{ s}^{-1} \Rightarrow \log \beta_{L_2Cu_3^*} = 16.9(8)$
	L'	$k_3 = 45(9) \text{ M}^{-1} \text{ s}^{-1}$ $k_{-3} = 9(2) \times 10^{-2} \text{ s}^{-1} \Rightarrow \log \beta_{L_2Cu_3^*} = 16.2(8)$
<i>Step 4</i>		
$L_2Cu_3^* \xrightleftharpoons[k_{-4}]{k_4} L_2Cu_3$	L	$k_4 = 2.0(4) \times 10^{-2} \text{ s}^{-1}$ $k_{-4} = 1.1(2) \times 10^{-2} \text{ s}^{-1} \Rightarrow \log \beta_{L_2Cu_3} = 17(1)$
	L'	$k_4 = 3(2) \times 10^{-2} \text{ s}^{-1}$ $k_{-4} = 2.7(2) \times 10^{-2} \text{ s}^{-1} \Rightarrow \log \beta_{L_2Cu_3} = 16.3(9)$
$L'Cu^* + L' \xrightleftharpoons[k_{-1}]{k_1} L'_2Cu$		$k_1 = 1.7(9) \times 10^3 \text{ M}^{-1} \text{ s}^{-1}$ $k_{-1} = 0.22(7) \text{ s}^{-1} \Rightarrow \log k_1/k_{-1} = 3.9(5)$
a) Solvent: MeCN/H ₂ O/CH ₂ Cl ₂ 80 : 15 : 5 (v/v); $T = 25.0(2)^\circ$; $I = 0.1$. b) Solvent: MeCN/CH ₂ Cl ₂ 1 : 1 (v/v); $T = 25.0(2)^\circ$; $I = 0.1$. The errors are given as 3σ .		

 Table 3. Variation of the Pseudo-First-Order Constants and the Absorbance for the Formation of the Cu^I Complexes of L' vs. $[Cu^I]^a$

$[L']_{\text{tot}} \times 10^3 \text{ [M]}$	$[Cu^I]_{\text{tot}} \times 10^3 \text{ [M]}$	$k_{2,\text{obs}} \text{ [s}^{-1}\text{]}$	$k_{3,\text{obs}} \text{ [s}^{-1}\text{]}$	$k_{4,\text{obs}} \text{ [s}^{-1}\text{]}$	$A_{2,0}$	$A_{2,\infty}$
2.9	0.423	–	0.12	0.033	0.1	–
2.9	0.546	1.297	0.105	0.029	0.1	–
2.9	0.706	1.223	–	–	0.11	–
6.5	0.908	–	0.125	0.032	–	–
5.2	1.539	–	0.117	0.031	–	0.338
8.5	2.000	0.698	0.152	0.036	0.34	0.57
12.2	2.234	0.723	0.154	0.036	–	0.331
6.5	2.269	0.601	0.138	0.038	0.205	–
8.5	4.000	0.773	–	–	0.3	–
6.5	4.539	0.638	–	–	0.2	–
6.5	9.077	0.932	–	–	0.18	0.242
8.5	10.000	0.795	–	–	–	–
a) Solvent: MeCN/CH ₂ Cl ₂ , 50 : 50 (v/v); $T = 25.0(2)^\circ$; $I = 0.1$; $l = 1 \text{ cm}$; $\lambda = 500 \text{ nm}$.						

Table 4. Global Stability Constants of Cu^I Complexes with Various Bipyridine Ligands

Ligand	log β	λ_{\max} [nm] (ϵ_{\max} [M ⁻¹ cm ⁻¹])	Solvent ^{a)}
 1	log $\beta_{L_1Cu} = 3.90$ log $\beta_{L_2Cu} = 6.8(1)$ 12.95 < log $\beta_{L_3Cu} < 14.2$	341 (2240) 438 (5200)	MeCN [58] H ₂ O [59–61]
 2	log $\beta_{L_1Cu} = 5.4$ log $\beta_{L_2Cu} = 10.2$ log $\beta_{L_3Cu} = 3.8$ log $\beta_{L_4Cu} = 9.3$ log $\beta_{L_5Cu} = 15.8$	345 (2100) 440 (5000) 450 (6140) – 455 (5570) 455 (6570)	MeCN [62] MeCN/CH ₂ Cl ₂ 50 : 50 [63] H ₂ O/CH ₂ Cl ₂ 50 : 50 [60][64]
 3	log $\beta_{L_2Cu} = 11.4$	483 (7130)	H ₂ O/CH ₂ Cl ₂ 50 : 50 [60][64]
 4	log $\beta_{L_1Cu} = 4.5$ log $\beta_{L_2Cu} = 8.6$	380 (3380) 500 (10750)	MeCN/CH ₂ Cl ₂ 50 : 50 [63]
 5		470 (7100)	MeCN/CH ₂ Cl ₂ 50 : 50 [65]
 6	log $\beta_{L_2Cu_2} = 14$	500 (15400)	MeCN/CH ₂ Cl ₂ 50 : 50 [63]
 7	log $\beta_{L_1Cu} = 6.9$	465 (4400)	MeCN [66] 533 (1600)
 8	log $\beta_{L_2Cu_3} = 20.0$	450 (15260)	MeCN/CH ₂ Cl ₂ 50 : 50 [63]

^{a)} Mixed solvent ratio expressed by volume (v/v).

data for Cu^I complexes formed with various bipy derivatives are presented in Table 4. The distribution curves in Fig. 4, a and b, show the highly favored formation of the L₂Cu₃ species, indicating appreciable positive cooperativity in agreement with the results obtained for L'₂Cu₃ [36].

Ligands **2**, **4**, **5**, **6**, and **8** were examined in the same solvent as **L'**. The stability constants of the monomeric cuprous complex with **4** (*Table 4*) and the corresponding **L'**Cu species (*Table 1*) are identical within experimental errors. The same observation holds for the dimeric complexes with **4** and **L'**. These observations suggest that the formation of these two Cu^I complexes of oligo(bipyridine) is not subject to increased steric hindrance compared to the corresponding species with the model ligand **4**. If we compare **L** and **L'**, no significant difference is observed in the stability of the Cu^I complexes within experimental errors (*Table 1*). These data do not reflect that **L** is bearing bulkier substituents than **L'** or that 5% H₂O was added to the solvent used for **L**.

The Cu^I complexes of bipy and its derivatives give a broad intense MLCT band ($d\pi \rightarrow \pi^*$) in the VIS (430–530 nm), [67–69]. The λ_{\max} and the absorptivity of this band strongly depend on the substituents attached to the bipy moiety [70], which affect the geometry of the Cu^I complexes, the Cu–N bond length, and the electronic properties of the N-atoms [70–72]. An electron-withdrawing substituent shifts the absorption band to a lower frequency, whereas an electron-donating substituent raises the frequency [73]. The steric bulk of the substituents may cause lengthening of the Cu–N bond, leading to the destabilization of metal complexes, resulting in a poor back-bonding, and a compensatory blue-shift of the MLCT maximum [73]. Taking into account the electronic effects of the CO₂Et and CONEt₂ substituents at C(4) and C(4') as well as the effects of the steric bulk of these substituents, one may conclude that the differences in the spectrophotometric properties of the Cu^I complexes of **8** and **L** are predominantly determined by steric effects, whereas both electronic and steric effects contribute when comparing the analogous complexes of **8** and **L'**. The electronic properties of the substituents could explain the observed blue shift of the MLCT bands of Cu^I complexes of **L'** and **L**, respectively (*Tables 1* and *4*).

The absorption spectra obtained for **LCu**, **L₂Cu₂**, and **L₂Cu₃** clearly indicate the coordination of two bipy units to the Cu centers. The only structure that can be proposed for **LCu** is, therefore, the coordination provided by a folded ligand **L**. The CH₂OCH₂ bridge is short enough to hinder tetrahedral binding of an ion by two consecutive bipy groups of the same ligand. We conclude that the Cu^I cation in **LCu** is coordinated by the two external bipy. Such a folded structure has already been observed for the Cu^I species formed with 2,2'-bis(2,2'-bipyridin-6-yl)biphenyl [66]. The two **L₂Cu₂** and **L₂Cu₃** species are expected to be of double-helicate type by analogy with the tricuprous species of its unsubstituted parent **8**, for which the double helicate structure was confirmed by X-ray crystallography [7]. The X-ray structure [65] of **L₂Cu₃** shows that the presence of the CO₂Et groups increases the stacking of the bipy groups and enhances the distortion of the tetrahedral coordination geometry compared to its unsubstituted analog. The variation of the electronic maxima then indicates that the stacking of the bipy units decreases between **L₂Cu₂** and **L₂Cu₃**. Moreover, the similarity of the stability constants related to **L₂Cu₂** and its corresponding analog with the ditopic ligand **6** (*Table 4*) in the same solvent could suggest that the structure of the two complexes is similar, and that the two Cu^I cations in **L₂Cu₂** occupy vicinal coordination sites. As a consequence, the third Cu^I cation would then coordinate to the free external binding sites (*Fig. 8*).

Formation Processes of Cu^I Complexes. The same formation process with four steps (*Table 2*) has been found for the formation of the tricuprous helicates **L₂Cu₃** (*Fig. 5*)

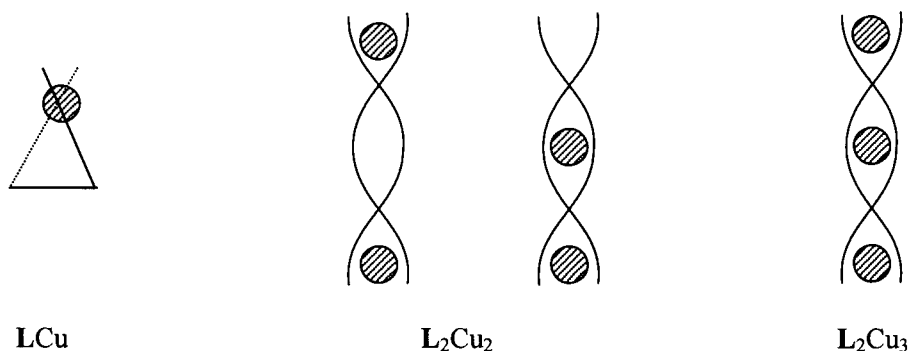


Fig. 8. Schematic representation of Cu^{I} complexes of **L**

and $\text{L}'_2\text{Cu}_3$ (Table 3). *Step 1*, which involves two Cu^{I} cations, leads to the formation of LCu_2^* . These reactions were too fast to be measured by a stopped-flow technique in agreement with the high values of the second-order-rate constant observed for the formation of the Cu^{I} (bipy) or Cu^{I} (6,6'-Me₂-bipy) complex (*ca.* $10^8 \text{ M}^{-1} \text{ s}^{-1}$) [62]. Fig. 6 shows an intense absorption band centered at 560 nm in the time-resolved spectra, and indicates the formation of kinetic intermediates* LCu^* and LCu_2^* , which do not have the same coordination geometry as the corresponding thermodynamic Cu^{I} species, displaying a different spectrophotometric behavior. A monomeric Cu^{I} complex with an open chain N₄ Schiff base ligand (1,8-bis(pyridin-2-yl)-2,7-diazaocta-1,7-diene) presents a spectrum, which was characterized by two absorption maxima at *ca.* 420 and 600 nm in MeCN [74]. The data for ϵ_{max} , which are sensitive to the solvent, strongly suggest the participation of the solvent to the inner coordination sphere of Cu^{I} . Two monomeric complexes combine in MeCN to form a binuclear helical complex, which allows an almost ideal tetrahedral coordination of each Cu^{I} [74]. These data suggest that, in our process (Fig. 6), the first reactive intermediate* could have a highly distorted coordination geometry, and that MeCN could participate to the inner coordination sphere.

The *Step 2* could be related to the addition of the second strand, which is two orders of magnitude lower than the second-order-rate constant measured for the formation of the Cu^{I} (6,6'-Me₂-bipy) complex ($2.7 \times 10^7 \text{ M}^{-1} \text{ s}^{-1}$) [62]. These data could be explained by steric effects. The rate constant is three times higher for **L** ($k_2 = 7(2) \times 10^5 \text{ M}^{-1} \text{ s}^{-1}$) than for **L'** ($k_2 = 2.0(5) \times 10^5 \text{ M}^{-1} \text{ s}^{-1}$). A slow binding of the second **L'** on $\text{L}'\text{Cu}^*$ was also observed in excess of ligand **L'** (Table 2). *Step 2* is slower, when the bulkiness of the substituents decreases. This result suggests that bulky substituents could prevent early concerted rearrangement and favor the formation of more reactive intermediates* with distorted coordination geometries, which will facilitate the approach of a second strand. If we consider the back reaction, L_2Cu_2^* dissociates *ca.* 100 times faster ($k_{-2} = 53.0(4) \text{ s}^{-1}$) than $\text{L}'_2\text{Cu}_2^*$ ($k_{-2} = 0.6(1) \text{ s}^{-1}$). These data agree well with our previous discussion and confirm the higher reactivity of the kinetic intermediate* L_2Cu_2^* compared to $\text{L}'_2\text{Cu}_2^*$.

Step 3 could be assigned to the complexation of the last Cu^{I} cation. The low rate-constant values observed for the Cu^{I} coordination leading to L_2Cu_3^* , $k_3 = 1.0(1) \times$

$10^3 \text{ M}^{-1} \text{ s}^{-1}$ and $45(9) \text{ M}^{-1} \text{ s}^{-1}$ for **L** and **L'**, respectively, reflects the difficulty of the cation to reach the coordination site due to the geometric organization of the ligands imposed by the complexation of the two first Cu^{I} . The difference between **L** and **L'** could also be due to the lower basicity of the bipy N-sites of **L'** due to the stronger electron-withdrawing effect of the ester group. The respective dissociation reactions of L_2Cu_3^* and $\text{L}'_2\text{Cu}_3^*$ are of the same order of magnitude and do not reflect any significant effect of the substituents on these intermediate structures*.

The last monomolecular step, independent of concentrations of Cu^{I} and ligand, is attributed to a final intracomplex rearrangement, which leads to the thermodynamic tricuprous helicates. The slow rearrangement rates are similar for L_2Cu_3^* ($2(2) \times 10^{-2} \text{ s}^{-1}$) and $\text{L}'_2\text{Cu}_3^*$ ($1.4(2) \times 10^{-2} \text{ s}^{-1}$).

Our spectrophotometric results at equilibrium are dominated by the formation of bis(bipy) coordination sites around Cu^{I} with the expected absorbances related to tetrahedral geometries. This trend could even lead to folded structures as suggested earlier [39]. The self-assembly process of the helicates L_2Cu_3 and $\text{L}'_2\text{Cu}_3$ goes *via* intermediates* with highly distorted coordination geometries, clearly reflected by absorption bands at 560 nm, which lead to a slow and final rearrangement of the helicates. For ligand **L'**, the activation parameters were calculated for *Steps 2, 3, and 4* ($\Delta S_2^\ddagger = 17 \text{ eu}$, $\Delta H_2^\ddagger = 5.3 \text{ kcal mol}^{-1}$, $\Delta G_2^\ddagger = 0.2 \text{ kcal mol}^{-1}$; $\Delta S_3^\ddagger = 4 \text{ eu}$, $\Delta H_3^\ddagger = 2.3 \text{ kcal mol}^{-1}$, $\Delta G_3^\ddagger = 1.1 \text{ kcal mol}^{-1}$; $\Delta S_4^\ddagger = 0.7 \text{ eu}$, $\Delta H_4^\ddagger = 2.1 \text{ kcal mol}^{-1}$, $\Delta G_4^\ddagger = 1.9 \text{ kcal mol}^{-1}$). These data show a decreasing entropic contribution along the process and a high activation energy for the rearrangement of the helicate $\text{L}'_2\text{Cu}_3$.

The mechanistic scheme is markedly complicated by the fact that the binding of two oligo(bipy) strands with Cu^{I} ions may yield both non-entangled 'side-by-side' and helical structures [75]. One could expect the formation of the first type to be kinetically faster than that of the second, where the ligands have to wrap around each other. Note also that stacking between the bipy subunits is only possible in the double helical form. Thus, one might suggest that the reactive kinetic intermediates* formed in the complexation process involve 'side-by-side'-type structures, with more or less distorted Cu^{I} coordination sites, which would then rearrange to the thermodynamically more stable, helical species. As a consequence, the last step, which occurs in a monomolecular fashion between species possessing both two strands and all three Cu^{I} centers, would correspond to such an internal rearrangement to the final fully double helical complex. *Fig. 9* presents a partial schematic illustration of this highly complicated situation.

Conclusion. – The present study has allowed to unravel at least partially, the kinetic and mechanistic processes occurring on formation of double helicates. It shows that such self-assembly processes, following a directing program [1], may involve highly complex routes towards the final encoded thermodynamic entity.

When the reactions become slow enough, intermediates* may be stable enough for isolation and characterization, as was the case in the formation of circular helicates, which is preceded by a kinetically favored triple helicate [76]. In a broader view, kinetic studies provide insight into the various steps and intermediates* of complex self-assembly processes, and, therefore, into the factors which influence the output entities. Such information is of much interest for progressively gaining control over the

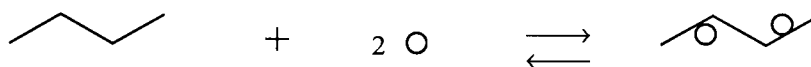
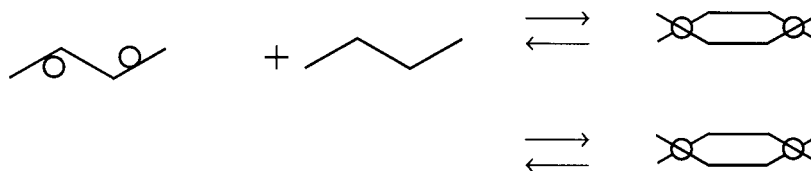
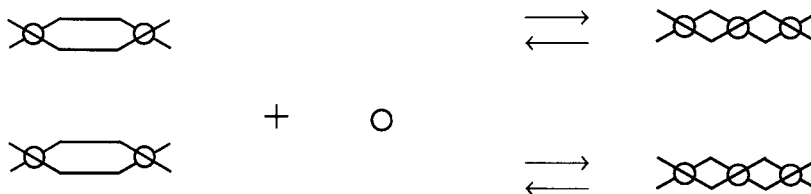
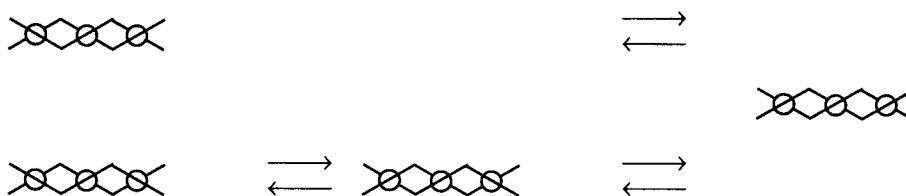
Step 1**Step 2****Step 3****Step 4**

Fig. 9. Schematic representation of the proposed mechanism

evolution of self-assembling systems by introducing suitable and robust instructions in the programming.

The authors thank Dr. A. Van Dorsselaer and Dr. E. Leize for the ES-MS spectra.

Supplementary Information Available. Table S1 listing ES-MS mass values, and Table S2, Table S3, and Fig. S1 presenting kinetic data.

REFERENCES

- [1] J.-M. Lehn, 'Supramolecular Chemistry: Concepts and Perspectives', VCH: Weinheim, 1995, Chapter 9, p. 139.
- [2] P. N. W. Baxter, in 'Comprehensive Supramolecular Chemistry', Eds. J. L. Atwood, J. E. D. Davies, D. D. MacNicol, F. Vögtle, J.-M. Lehn, Pergamon, Oxford, 1996, Vol. 9, Chapt. 5, . 165; E. C. Constable, in 'Comprehensive Supramolecular Chemistry', Eds. J. L. Atwood, J. E. D. Davies, D. D. MacNicol, F. Vögtle, J.-M. Lehn, Pergamon, Oxford, 1996, Vol. 9, Chapt. p. 213; M. Fujita, in 'Comprehensive Supramolecular Chemistry', Eds. J. L. Atwood, J. E. D. Davies, D. D. MacNicol, F. Vögtle, J.-M. Lehn, Pergamon, Oxford, 1996, Vol. 9, Chapt. 7, p. 253.
- [3] D. S. Lawrence, T. Jiang, M. Levett, *Chem. Rev.* **1995**, *95*, 2229; R. F. Saalfrank, *Curr. Opin. Solid State Mat. Sci.* **1998**, *3*, 407; B. Olenyuk, A. Fechtenkotter, P. J. Stang, *J. Chem. Soc., Dalton Trans.* **1998**, *11*, 1707; M. Fujita, *Polym. Mater. Sci. Eng.* **1999**, *80*, 27, D. L. Caulder, K. N. Raymond, *J. Chem. Soc., Dalton Trans.* **1999**, *8*, 1185; C. Piguet, *J. Inclusion Phenom. Macrocycl. Chem.* **1999**, *34*, 361; S. Leininger, B. Olenyuk, P. J. Stang, *Chem. Rev.* **2000**, *100*, 853; G. F. Swiegers, T. J. Malefetse, *Chem. Rev.* **2000**, *100*, 3483.
- [4] A. Williams, *Chem. Eur. J.* **1997**, *3*, 15.
- [5] J.-M. Lehn, *Chem. Eur. J.* **2000**, *6*, 2097.
- [6] C. Piguet, G. Bernardinelli, G. Hopfgartner, *Chem. Rev.* **1997**, *97*, 2005; E. C. Constable, *Tetrahedron* **1992**, *48*, 10013.
- [7] J.-M. Lehn, A. Rigault, J. Siegel, J. Harrowfield, B. Chevrier, D. Moras, *Proc. Natl. Acad. Sci. U.S.A.* **1987**, *84*, 2565.
- [8] J.-M. Lehn, A. Rigault, *Angew. Chem., Int. Ed.* **1988**, *27*, 1095.
- [9] D. Zurita, P. Baret, J. L. Pierre, *New J. Chem.* **1994**, *18*, 1143.
- [10] C. Piguet, J. C. Bünzli, G. Bernardinelli, C. F. Bochet, P. Froidevaux, *J. Chem. Soc., Dalton Trans.* **1995**, 83.
- [11] A. T. Baker, D. C. Graig, G. Dong, *Inorg. Chem.* **1996**, *35*, 1091.
- [12] A. K. Duhme, Z. Dauter, R. C. Hider, S. Pohl, *Inorg. Chem.* **1996**, *35*, 3059.
- [13] E. J. Enemark, T. D. P. Stack, *Inorg. Chem.* **1996**, *35*, 2719.
- [14] E. C. Constable, F. Heirtzler, M. Neuberger, M. Zehner, *J. Am. Chem. Soc.* **1997**, *119*, 5606.
- [15] K. T. Potts, M. P. Wentland, D. Ganguly, G. D. Storrer, S. K. Cha, J. Cha, H. D. Abruña, *Inorg. Chim. Acta* **1999**, *288*, 189.
- [16] S. M. Couchman, J. C. Jeffery, M. D. Ward, *Polyhedron* **1999**, *18*, 2633.
- [17] P. N. W. Baxter, G. S. Hanan, J.-M. Lehn, *Chem. Commun.* **1996**, 2019.
- [18] See for instance: M.-T. Youinou, N. Rahmouni, J. Fischer, J. A. Osborn, *Angew. Chem., Int. Ed.* **1992**, *31*, 733; P. N. W. Baxter, J.-M. Lehn, J. Fischer, M.-T. Youinou, *Angew. Chem., Int. Ed.* **1994**, *33*, 2284; A. M. Garcia, F. J. Romero-Salguero, D. M. Bassani, J.-M. Lehn, G. Baum, D. Fenske, *Chem. Eur. J.* **1999**, *5*, 1803; G. S. Hanan, D. Volkmer, U. S. Schubert, J.-M. Lehn, G. Baum, D. Fenske, *Angew. Chem., Int. Ed.* **1997**, *36*, 1842.
- [19] B. Hasenknopf, J.-M. Lehn, B. O. Kneisel, G. Baum, D. Fenske, *Angew. Chem., Int. Ed.* **1996**, *35*, 1838; B. Hasenknopf, J.-M. Lehn, N. Boumediene, A. Dupont-Gervais, A. Van Dorsselaer, B. Kneisel, D. Fenske, *J. Am. Chem. Soc.* **1997**, *119*, 10956.
- [20] P. N. W. Baxter, J.-M. Lehn, A. De Cian, J. Fischer, *Angew. Chem., Int. Ed.* **1993**, *32*, 69; P. N. W. Baxter, J.-M. Lehn, G. Baum, D. Fenske, *Chem. Eur. J.* **1999**, *5*, 102; P. N. W. Baxter, J.-M. Lehn, B. O. Kneisel, G. Baum, D. Fenske, *Chem. Eur. J.* **1999**, *5*, 113.
- [21] C. O. Dietrich-Buchecker, J. P. Sauvage, 'Bioorg. Chem. Front.', Ed. H. Dugas, Springer-Verlag, Berlin, 1991, Vol. 2, p. 146.
- [22] J. C. Chambron, C. O. Dietrich-Buchecker, J. P. Sauvage, in 'Comprehensive Supramolecular Chemistry', Eds. J. P. Sauvage, M. W. Hosseini, Pergamon, Oxford, 1996, Vol. 9, Chapter 2, p. 43.
- [23] D. B. Amabilino, J. F. Stoddart, *Chem. Rev.* **1995**, *95*, 2725.

- [24] B. Hasenknopf, J.-M. Lehn, *Helv. Chim. Acta* **1996**, *79*, 1643.
- [25] R. Krämer, J.-M. Lehn, A. DeCian, J. Fischer, *Angew. Chem., Int. Ed.* **1993**, *32*, 703.
- [26] C. Piguët, G. Hopfgartner, B. Bocquet, O. Schaad, A. F. Williams, *J. Am. Chem. Soc.* **1994**, *116*, 9092; V. C. M. Smith, J.-M. Lehn, *Chem. Commun.* **1996**, 2733.
- [27] B. Hasenknopf, J.-M. Lehn, G. Baum, D. Fenske, *Proc. Natl. Acad. Sci. U.S.A.* **1996**, *93*, 1397.
- [28] V. A. Grillo, E. J. Seddon, C. M. Grant, G. Aromi, J. C. Bollinger, K. Foltling, G. Christou, *Chem. Commun.* **1997**, 1561; W. Dai, H. Hu, X. Wei, S. Zhu, D. Wang, K. Yu, K. Dalley, X. Kou, *Polyhedron* **1997**, *16*, 2059; C. Piguët, G. Hopfgartner, B. Bocquet, O. Schaad, A. F. Williams, *J. Am. Chem. Soc.* **1994**, *116*, 9092.
- [29] D. P. Funeriu, Y. B. He, H. J. Bister, J.-M. Lehn, *Bull. Soc. Chim. Fr.* **1996**, *133*, 673; B. Kersting, M. Meyer, R. E. Powers, K. N. Raymond, *J. Am. Chem. Soc.* **1996**, *30*, 7221.
- [30] M. Jaquinod, E. Leize, N. Potier, A. M. Albrecht, A. Shanzer, A. Van Dorsselaer, *Tetrahedron Lett.* **1993**, *34*, 2771; G. Hopfgartner, C. Piguët, J. D. Henion, A. F. Williams, *Helv. Chim. Acta* **1993**, *76*, 1759; G. Hopfgartner, C. Piguët, J. D. Henion, *J. Am. Soc. Mass Spectrom.* **1994**, 748.
- [31] G. Hopfgartner, C. Piguët, J. D. Henion, A. F. Williams, *Helv. Chim. Acta* **1993**, *76*, 1759.
- [32] M. Greenwald, M. Eassa, E. Katz, I. Willner, Y. Cohen, *J. Electroanal. Chem.* **1997**, *434*, 77.
- [33] A. Marquis-Rigault, A. Dupont-Gervais, P. N. W. Baxter, A. Van Dorsselaer, J.-M. Lehn, *Inorg. Chem.* **1996**, *35*, 2307.
- [34] C. Piguët, G. Bernardinelli, B. Bocquet, A. Quattropani, A. F. Williams, *J. Am. Chem. Soc.* **1992**, *114*, 7440.
- [35] C. Piguët, J. C. Bünzli, G. Bernardinelli, C. G. Bochet, P. Froidevaux, *J. Chem. Soc., Dalton Trans.* **1995**, 83; S. Petoud, J. C. Bünzli, F. Renaud, C. Piguët, K. J. Schenk, G. Hopfgartner, *Inorg. Chem.* **1997**, *36*, 5750.
- [36] A. Pfeil, J.-M. Lehn, *J. Chem. Soc., Chem. Commun.* **1992**, 838.
- [37] T. M. Garrett, U. Koert, J.-M. Lehn, *J. Phys. Org. Chem.* **1992**, *5*, 529.
- [38] S. Blanc, P. Yakirevitch, E. Leize, M. Meyer, J. Libman, A. Van Dorsselaer, A. M. Albrecht-Gary, A. Shanzer, *J. Am. Chem. Soc.* **1997**, *119*, 4934.
- [39] A. Marquis-Rigault, A. Dupont-Gervais, A. Van Dorsselaer, J.-M. Lehn, *Chem. Eur. J.* **1996**, *2*, 1395.
- [40] N. Fatin-Rouge, S. Blanc, E. Leize, A. Van Dorsselaer, P. Baret, J.-L. Pierre, Albrecht-Gary, *Inorg. Chem.* **2000**, *39*, 5771.
- [41] M. M. Harding, U. Koert, J.-M. Lehn, A. Marquis-Rigault, C. Piguët, J. Siegel, *Helv. Chim. Acta* **1991**, *74*, 594.
- [42] R. Krämer, J.-M. Lehn, A. Marquis-Rigault, *Proc. Natl. Acad. Sci. U.S.A.* **1993**, *90*, 5394.
- [43] H. Meerwein, V. Hederich, K. Wunderlich, *Ber. Dtsch. Pharm. Ges.* **1958**, *63*, 548.
- [44] L. G. Sillen, *Acta Chem. Scand.* **1964**, *18*, 1085.
- [45] L. G. Sillen, B. Warnqvist, *Ark. Kemi.* **1968**, *31*, 377.
- [46] J. Havel, *Pure Appl. Chem.* **1972**, *34*, 370.
- [47] H. Gampp, M. Maeder, C. J. Meyer, A. D. Zuberbühler, *Talanta* **1985**, *32*, 95.
- [48] F. J. C. Rossoti, H. S. Rossoti, R. J. Whewell, *J. Inorg. Nucl. Chem.* **1971**, *33*, 2051.
- [49] H. Gampp, M. Maeder, C. J. Meyer, A. D. Zuberbühler, *Talanta* **1985**, *32*, 257.
- [50] H. Gampp, M. Maeder, C. J. Meyer, A. D. Zuberbühler, *Talanta* **1986**, *33*, 943.
- [51] D. W. Marquardt, *J. Soc. Ind. Appl. Math.* **1963**, *11*, 431.
- [52] M. Maeder, A. D. Zuberbühler, *Anal. Chem.* **1990**, *62*, 2220.
- [53] Bio-Logic Company, Ed. Bio-Logic Company, Echirolles, 1991.
- [54] J. A. Nelder, R. Mead, *The Computer Journal* **1965**, *7*, 308.
- [55] E. Yeramian, P. Claverie, *Nature* **1987**, *326*, 169.
- [56] J. Leatherbarrow, Ed. Biosoft, Cambridge, 1987.
- [57] N. Ingri, W. Kakolowicz, L. G. Sillen, B. Warnqvist, *Talanta* **1967**, *14*, 1261.
- [58] P. Leupin, Ph.D. Thesis, Université de Fribourg, Switzerland, 1980.
- [59] E. I. Onstott, H. A. Laitinen, *J. Chem. Soc.* **1950**, 4724.
- [60] B. R. James, J. P. Williams, *J. Chem. Soc.* **1961**, 2007.
- [61] G. Anderreg, *Helv. Chim. Acta* **1963**, *46*, 2397.
- [62] U. Ochsenbein, Ph.D. Thesis, Université de Fribourg, Switzerland, 1981.
- [63] A. Pfeil, J.-M. Lehn, unpublished results.
- [64] B. R. James, M. Parris, J. P. Williams, *J. Chem. Soc.* **1961**, 4630.
- [65] A. Rigault, Ph.D. Thesis, Université Louis Pasteur de Strasbourg, France, 1992.
- [66] E. Muller, C. Piguët, G. Bernardinelli, A. F. Williams, *Inorg. Chem.* **1988**, *27*, 849.
- [67] R. J. P. Williams, *J. Chem. Soc.* **1955**, 137.
- [68] R. A. Palmer, T. S. Piper, *Inorg. Chem.* **1966**, *5*, 864.

- [69] W. R. McWinnie, J. D. Miller, *Adv. Inorg. Chem. Radiochem.* **1969**, *12*, 135.
- [70] S. Kitakawa, M. Munakata, A. Hitgashie, *Inorg. Chim. Acta* **1984**, *5*, 79.
- [71] S. Kitakawa, M. Munakata, A. Hitgashie, *Inorg. Chim. Acta* **1982**, *59*, 219.
- [72] C. C. Phiher, D. R. McMillin, *Inorg. Chem.* **1986**, *5*, 1329.
- [73] C. S. Tsai, *Can. J. Chem.* **1967**, *45*, 2862.
- [74] J. Lange, H. Elias, H. Paulus, J. Muller, U. Weser, *Inorg. Chem.* **2000**, *39*, 3342.
- [75] W. Zarges, J. Hall, J.-M. Lehn, *Helv. Chim. Acta* **1991**, *74*, 1843.
- [76] B. Hasenknopf, J.-M. Lehn, N. Boumediene, M. Leize, A. Van Dorsselaer, *Angew. Chem., Int. Ed.* **1998**, *37*, 3265.

Received May 14, 2001